

Probing the Missing Link between the Diffuse Interstellar Bands and the Total-to-Selective Extinction Ratio R_V – I. Extinction versus Reddening

Kaijun Li^{1,2}, Aigen Li^{2*}, and F.Y. Xiang^{1,2†}

¹ *Department of Physics, Xiangtan University, 411105 Xiangtan, Hunan Province, China*

² *Department of Physics and Astronomy, University of Missouri, Columbia, MO 65211, USA*

Received date / Accepted date

ABSTRACT

The carriers of the still (mostly) unidentified diffuse interstellar bands (DIBs) have been a long-standing mystery ever since their first discovery exactly 100 years ago. In recent years, the ubiquitous detection of a large number of DIBs in a wide range of Galactic and extragalactic environments has led to renewed interest in connecting the occurrence and properties of DIBs to the physical and chemical conditions of the interstellar clouds, with particular attention paid to whether the DIB strength is related to the shape of the interstellar extinction curve. To shed light on the nature and origin of the DIB carriers, we investigate the relation between the DIB strength and R_V , the total-to-selective extinction ratio, which characterizes how the extinction varies with wavelength (i.e., the shape of the extinction curve). We find that the DIB strength and R_V are not related if we represent the strength of a DIB by its reddening-normalized equivalent width (EW), in contrast to the earlier finding of an anticorrelation in which the DIB strength is measured by the extinction-normalized EW. This raises a fundamental question about the appropriate normalization for the DIB EW. We argue that the hydrogen column density is a more appropriate normalization than extinction and reddening.

Key words: ISM: dust, extinction — ISM: lines and bands — ISM: molecules

1 INTRODUCTION

The enigmatic “diffuse interstellar bands” (DIBs) are a set of over 600 non-stellar absorption features observed in starlight crossing interstellar clouds, spanning the wavelength range of the near ultraviolet (UV) at $\lambda \gtrsim 4000$ Å to the near infrared (IR) at $\lambda \lesssim 1.8$ μm (e.g., see Sarre 2006). It is frustrating that, except five DIBs were recently identified as due to C_{60}^+ ,¹ the vast majority of DIBs have not yet been firmly identified,

despite an extensive observational, experimental, theoretical and computational exploration of an entire century — it has been exactly 100 years since the first serendipitous detection of two DIBs (at 5780 and 5797 Å) by Mary Lea Heger, then a graduate student at Lick Observatory (see Heger 1922), although their interstellar origin was not firmly established until 15 years later by Merrill (1934).

Nevertheless, in recent years much progress has been made in detecting a large number of DIBs in a wide variety of Galactic interstellar environments, ranging from sight-lines toward diffuse clouds, translucent clouds, molecular clouds, bright reflection nebulae, giant H II regions, massive star forming regions, massive young stellar clusters, and the Galactic center (see Snow & McCall 2006, Hobbs et al. 2008, 2009, Cox 2011, Cami & Cox 2014, Krełowski 2018, Sonnen-trucker et al. 2018). The detection of DIBs in extragalactic environments has also been reported (see Cordiner 2014), ranging from the Local Group galaxies including the Large and Small Magellanic Clouds (Ehrenfreund et al. 2002; Cox et al. 2006, 2007; Welty et al. 2006; van Loon et al. 2013), M31 (Cordiner et al. 2008b, 2011), M33 (Cordiner et al.

* E-mail: lia@missouri.edu

† E-mail: fyxiang@xtu.edu.cn

¹ Campbell et al. (2015, 2016) and Walker et al. (2015) measured the gas-phase spectrum of C_{60}^+ at ultra-low temperatures and found that the spectral characteristics of gas-phase C_{60}^+ are in agreement with five DIBs at 9348.4, 9365.2, 9427.8, 9577.0, and 9632.1 Å (Cordiner et al. 2019), supporting the earlier assignment of the 9577 and 9632 Å DIBs to C_{60}^+ (Foing & Ehrenfreund 1994) which was based on the absorption spectrum recorded in a neon matrix (Fulara et al. 1993). Omont (2016) further proposed that fullerenes of various sizes with endohedral or exohedral inclusions and heterofullerenes could be viable DIB carrier candidates.

2008a), M 82 (Welty et al. 2014), and the Antennae galaxies (Monreal-Ibero et al. 2018), to more distant starburst galaxies (Heckman & Lehnert 2000), host galaxies of Type Ia supernovae (Sollerman et al. 2005, Cox & Patat 2008, Phillips et al. 2013), interacting spiral galaxies (Monreal-Ibero et al. 2015), intervening absorption systems toward quasars (Ellison et al. 2008) and damped Ly α absorbers at cosmological distances (DLAs; Junkkarinen et al. 2004, York et al. 2006, Lawton et al. 2008).

Motivated by the ubiquitous detection of DIBs in various Galactic and extragalactic environments, in recent years much effort has been devoted to exploring whether and how the presence, strengths, and spectral profiles of DIBs are affected by the physical and chemical conditions of the interstellar environments (e.g., see Ruiterkamp et al. 2005, Cox et al. 2006, Cox & Spaans 2006, Vos et al. 2011, Xiang et al. 2011, Kos & Zwitter 2013, Clayton 2014, Sonnentrucker 2014). There is a rich literature on DIB profiles and their variations in different lines of sight. A number of the DIBs (including those at 5780, 5797, and 6284 Å) seen toward stars in the Orion Trapezium region are both broadened and shifted to the red (Porceddu et al. 1992). Blueshifted DIBs (e.g., those at 5797 and 6614 Å) which are broader than usual and whose red wings are more prominent than usual are seen toward the runaway star HD 34078 (Galazutdinov et al. 2006) which is currently interacting with a diffuse molecular cloud (Boissé et al. 2009). Anomalously broad DIBs at 5780, 5797, 6196, and 6614 Å with remarkable extended tails toward red are found in absorption along the line of sight to Herschel 36, an O star multiple system illuminating the bright Hourglass nebula of the H II region Messier 8 (Dahlstrom et al. 2013, York et al. 2014).

In addition to the environmental variations of the DIB spectral profiles, the strength of a DIB, as measured by its equivalent width (EW), is also known to vary significantly from sightline to sightline. This variation appears to depend on the local environmental conditions (see Cami & Cox 2014 and references therein).² It has long been known that the DIB strength correlates with the interstellar reddening $E(B - V)$ caused by solid dust particles³ — as a matter of fact, this correlation was one of the principal arguments supporting an interstellar origin of DIBs (Merrill 1934). Although the correlation between the DIB strength and the interstellar reddening does not necessarily mean that the interstellar reddening and DIBs share a common carrier — it may merely reflect the fact that the DIB carriers are well mixed with dust and gas in interstellar clouds so that both the amount of DIB carriers and the quantity of interstellar dust grains are linearly proportional to the amount of interstellar gas along the line of sight. Nevertheless, the DIB carriers and interstellar dust grains could be physically related, e.g., the latter could protect the former from photodestruction by shielding the former from the UV starlight.

² For example, DIBs were observed to be weaker by factors of ~ 2 or more on a per unit reddening basis in photon-dominated regions (PDR; see Jenniskens et al. 1994).

³ Also known as the “color excess”, the interstellar reddening is defined as the extinction difference between two wavebands, e.g., $E(B - V) = A_B - A_V$ is the difference between the B -band extinction (A_B) at $\lambda \approx 4400$ Å and that of the V -band (A_V) at $\lambda \approx 5500$ Å.

In this context, it would be of great value to explore how the DIB strength varies with $R_V \equiv A_V/E(B - V)$, the total-to-selective extinction ratio, which characterizes the steepness of the UV extinction: for lines of sight with a smaller R_V , the UV extinction often increases more steeply with λ^{-1} , the inverse wavelength (e.g., see Figures 4,6 of Cardelli, Clayton & Mathis 1989, hereafter CCM). On a per unit A_V basis, a smaller R_V implies a more severe attenuation of the UV radiation and thus a more effective protection of the DIB carriers. While this scenario is complicated by the fact that those lines of sight with a smaller R_V often subject to a smaller amount of visual extinction (A_V), observationally, this has been demonstrated in the σ Sco cloud toward HD 147165 (for which $R_V \approx 4.25$, Lewis et al. 2005) and the ζ Oph cloud toward HD 149757 (for which $R_V \approx 3.08$, Fitzpatrick & Massa 2007). While the interstellar reddening [$E(B - V) \approx 0.34$ for σ Sco and $E(B - V) \approx 0.32$ for ζ Oph] is similar for these two clouds, the 5780 Å DIB of σ Sco is substantially stronger than that of ζ Oph. However, it is worth noting that the strengths of the 5797 Å DIB of these very same two clouds are nearly identical (Krelowski & Westerlund 1988). The effects of the UV starlight on the DIB strength has also been observationally studied by Cami et al. (1997) and Sonnentrucker et al. (1997) for a larger number of DIBs and a larger sample of sightlines.

To shed light on the physical and chemical nature of the still unidentified DIB carriers, we have initiated a program to explore the possible relations between the DIB strengths and the various interstellar parameters (e.g., extinction, UV radiation, and gas densities). In this work, we quantitatively examine how DIBs vary with R_V , first for the sightlines toward the H II region in M17 and then for a larger sample (§2). It is found that the DIB strength, measured as $EW/E(B - V)$, the EW of a DIB normalized by reddening, is not correlated with R_V . This is in contrast to the earlier finding of an anticorrelation made by Ramírez-Tannus et al. (2018) who normalized the DIB EW by A_V . The results are discussed in §3 and summarized in §4.

2 IS THE DIB STRENGTH RELATED TO R_V ?

Following Ramírez-Tannus et al. (2018), we first consider the prominent DIBs seen in M17, a giant H II region. Located in the Carina-Sagittarius spiral arm of the Galaxy at a distance of ~ 1.98 kpc, M17 is one of the brightest and best-studied giant H II region (Hoffmeister et al. 2008, Povich et al. 2009, Ramírez-Tannus et al. 2017). M17 is selected for this study because the sightlines toward M17 exhibit a significant spread in both extinction ($A_V \sim 3$ –15 mag) and R_V (~ 2.8 –5.5). Hanson et al. (1997) investigated the behavior of the DIBs along the sightlines toward M17, over such a wide extinction range. They found that the DIBs show little change in spectral shape. Ramírez-Tannus et al. (2018) obtained the 300–2500 nm spectra of 11 pre-main sequence OB stars with the X-shooter Spectrograph mounted on the ESO Very Large Telescope (VLT). They determined the reddening, visual extinction, and R_V for the lines of sight toward these stars. They also measured the EWs of 14 prominent DIBs for most of these sightlines. As tabulated in Table 1, we adopt the reddening $E(B - V)$, R_V , and DIB EW data of Ramírez-Tannus et al. (2018) and examine the correlation

between the DIB EW and R_V^{-1} in M17. For different lines of sight crossing different amounts of interstellar matter, the DIB EW is expected to correlate with $E(B-V)$.⁴ Therefore, to cancel out the common correlation between the DIB EW and $E(B-V)$ among the various lines of sight, we normalize the DIB EWs by $E(B-V)$. We perform a correlation analysis between the reddening-normalized EWs of 14 DIBs, $EW/E(B-V)$, and R_V^{-1} for the lines of sight toward M17. As shown in Figure 1, for all 14 DIBs at 4430, 5780, 5797, 6196, 6284, 6379, 6614, 7224, 8620, 9577, 9632, 11797, 13176, and 15268 Å, the Pearson correlation coefficient r never exceeds 0.50, indicating that $EW/E(B-V)$ and R_V^{-1} are not correlated.⁵ This is also supported by the Kendall’s τ test (see Figure 1).

We have also performed the Pearson correlation analysis and the Kendall’s τ test for six of these 14 DIBs for a large sample of 97 sightlines of which both EWs and R_V have been compiled from the literature by Xiang et al. (2017). As illustrated in Figure 2, no correlation is found between $EW/E(B-V)$ and R_V^{-1} .

3 DISCUSSION

Ramírez-Tannus et al. (2018) investigated the correlation between EW/A_V , the extinction-normalized DIB EWs, and R_V^{-1} for the 14 prominent DIBs seen in M17. As reproduced here in Figure 3, it is apparent that, with the Pearson correlation coefficient r exceeding 0.80 for five of the 14 DIBs and exceeding 0.60 for 10 of the 14 DIBs, EW/A_V appears to correlate with R_V^{-1} for the vast majority of the DIBs seen in M17. This is in stark contrast to our finding that there seems to be no correlation between $EW/E(B-V)$ and R_V^{-1} (see §2).

The major difference between our approach and that of Ramírez-Tannus et al. (2018) lies in the normalization: while we normalize the DIB EW by reddening $E(B-V)$, Ramírez-Tannus et al. (2018) took the visual extinction A_V as the normalization. We argue that the anticorrelation between EW/A_V and R_V^{-1} may be related to the fact that, for the M17 sample of Ramírez-Tannus et al. (2018), A_V and R_V are themselves correlated. As shown in Figure 3(o), with a Pearson correlation coefficient of $r \approx -0.84$ and a Kendall correlation coefficient of $\tau \approx -0.79$ and a corresponding probability $p \approx 0.0065$ of a chance correlation, an anticorrelation between A_V and R_V^{-1} is apparent.⁶ Therefore, even

if DIBs do not correlate with R_V at all, the intrinsic anticorrelation between A_V and R_V^{-1} would lead to EW/A_V to correlate with R_V^{-1} . On the other hand, as demonstrated in Figure 1(o), $E(B-V)$ is not related to R_V^{-1} .

This raises a fundamental question: when one explores the possible relations between DIBs and other interstellar parameters or among different DIBs, what is a more appropriate normalization, A_V or $E(B-V)$? At a first glance, A_V appears to be a better normalization since A_V is a direct tracer of the dust column density. However, $E(B-V)$ is a better discriminator of dust size and therefore of R_V (e.g., see Figures 22.7, 22.8 of Draine 2011) in the sense that larger grains intend to be “grayer” and have larger R_V . When correlating the DIB EW with R_V , it thus seems more appropriate to normalize the DIB EW with $E(B-V)$ than A_V . In this way, any intrinsic relation between $E(B-V)$ and R_V would have been cancelled out. Also, it is well known and can be easily verified with the DIB EW data available in the public domain⁷ that the DIB strengths for most of the strong DIBs (e.g., those at 4430, 5780, 5797, 6284, 6613 Å) are more strongly correlated with $E(B-V)$ than with A_V . This appears to support $E(B-V)$ as a more favorable normalization than A_V . On the other hand, this could also be considered as evidence for supporting that DIBs actually physically anticorrelate with R_V , at least through the so-called “skin” or “edge” effect (Snow & Cohen 1974), i.e., in dense molecular clouds characterized by larger-than-average R_V values, DIBs are weak or even completely absent at the cloud cores but grow in strength toward the cloud edges. This is possibly caused by the accretion of the DIB carriers onto the surfaces of large dust grains under conditions which favor dust growth in dense molecular clouds. As a result, DIB carriers are relatively under-abundant and thus many DIBs exhibit smaller strengths in these environments, i.e., places where dust with larger values of R_V typically resides.⁸

We argue that neither A_V nor $E(B-V)$ is an accurate tracer of the dust column density since both quantities involve the properties (e.g., size, composition) of the dust along the line of sight which exhibit regional variations. We suggest the hydrogen column density (N_H) is a more appropriate normalization than A_V and $E(B-V)$ since N_H directly measures the amount of interstellar material along a given sightline, while both A_V and $E(B-V)$ are actually only used as proxies for N_H . Unfortunately, in the literature there is no N_H information for the M17 sightlines of interest

⁴ In the ISM, dust and gas are well mixed as indicated by the relatively constant gas-to-extinction ratio, $N_H/E(B-V) \approx 5.8 \times 10^{21} \text{ H cm}^{-2} \text{ mag}^{-1}$ (Bohlin et al. 1978). Therefore, any two interstellar quantities that depend on either the amount of dust or the amount of gas in the line of sight will tend to, to some extent, correlate with each other. To explore the correlation between the DIB strength and the extinction parameters, the common dependence on the reddening $E(B-V)$ has to be cancelled out (e.g., see Witt et al. 1983, Xiang et al. 2011).

⁵ Although somewhat arbitrary, we suggest that, for two variables to be considered to be (even weakly) correlated, the Pearson correlation coefficient (r) should at least exceed 0.5 (e.g., see <https://explorable.com/statistical-correlation>).

⁶ Ramírez-Tannus et al. (2018) determined A_V and $E(B-V)$ by comparing the observed magnitudes of the target stars to the intrinsic ones of the same spectral type, i.e., $A_V = V - V_0$, and

$E(B-V) = (B-V) - (B-V)_0$. They derived R_V using the relation reported in Fitzpatrick & Massa (2007): $R_V \approx -0.26 + 1.19(A_V - A_K)/(A_B - A_V)$, where A_K is the K -band extinction. This explains why the Pearson correlation coefficient r between A_V and R_V^{-1} is not -1 which should have been the case if R_V was derived directly from $A_V/E(B-V)$.

⁷ See, e.g., the University of Chicago DIB database at <http://dib.uchicago.edu/public/index.html>.

⁸ Indeed, Hansen et al. (1997) have already noted that the DIBs observed in the direction of M17, over the extinction range of $A_V = 3\text{--}10 \text{ mag}$, does not show any significant increase in strength. They suggested that either the DIB features are already saturated at a small value of A_V , or that the interstellar material local to M17, where the increased extinction is being traced, does not contain DIB carriers.

here. This prevents us from a quantitative analysis of the relation between EW/N_H and R_V^{-1} .

4 SUMMARY

We have examined the relation between the DIB strength and R_V which characterizes how the extinction varies with wavelength, first for 14 DIBs in eight lines of sight toward young OB stars in the giant H II region M17 and then for six of these 14 DIBs in a large sample of 97 lines of sight compiled from the literature. It is found that the DIB strength, measured as the reddening-normalized DIB EW, is not correlated with R_V , in contrast to the earlier finding of an anticorrelation between the extinction-normalized DIB EW and R_V . We argue that, when comparing the DIB EW with R_V , neither A_V nor $E(B - V)$ is an ideal normalization since A_V is usually intrinsically higher for regions with larger R_V (i.e., $A_V \propto R_V$) while $E(B - V)$ preferably probes the surface layers of dense molecular cloud cores. We suggest that the really appropriate normalisation for the DIB EW, on physical grounds, would be N_H , the hydrogen column density.

ACKNOWLEDGEMENTS

We thank the anonymous referee for his/her very helpful comments and suggestions which have considerably improved the presentation of this work. KJL and FYX are supported in part by the Joint Research Funds in Astronomy (U1731106, U1731107 and U1531108) under cooperative agreement between the National Natural Science Foundation of China and Chinese Academy of Sciences. AL is supported in part by NSF AST-1816411.

REFERENCES

- Bohlin, R. C., Savage, B. D., & Drake, J. F. 1978, *ApJ*, 224, 132
 Boissé, P., Rollinde, E., Hily-Blant, P., et al. 2009, *A&A*, 501, 221
 Cami, J., Sonnentrucker, P., Ehrenfreund, P., & Foing, B.H. 1997, *A&A* 326, 822
 Cardelli, J. A., Clayton, G. C., & Mathis, J. S. 1989, *ApJ*, 354, 245
 Cami, J., & Cox, N.L.J. 2014, ed., *IAU Symp. 297, The Diffuse Interstellar Bands*, Cambridge Univ. Press
 Campbell, E.K., Holz, M., Gerlich, D., & Maier, J.P. 2015, *Nature*, 523, 322
 Campbell, E.K., Holz, M., & Maier, J.P. 2016, *ApJL*, 826, L4
 Clayton, G. C. 2014, in *IAU Symp. 297, The Diffuse Interstellar Bands*, ed. J. Cami & N. L. J. Cox (Cambridge: Cambridge Univ. Press), 147
 Cordiner, M. A. 2014, in *IAU Symp. 297, The Diffuse Interstellar Bands*, ed. J. Cami & N. L. J. Cox (Cambridge: Cambridge Univ. Press), 41
 Cordiner, M. A., Cox, N. L. J., Trundel, R., Evans, C. J., Hunter, I., Przybilla, N., Bresolin, F., & Salama, F. 2008a, *A&A*, 480, 13
 Cordiner, M. A., Smith, K. T., Cox, N. L. J., Evans, C. J., Hunter, I., Przybilla, N., Bresolin, F., & Sarre, P. J. 2008b, *A&A*, 492, L5
 Cordiner, M. A., Cox, N. L. J., Evans, C. J., Trundle, C., Smith, K. T., Sarre, P. J., & Gordon, K. D. 2011, *ApJ*, 726, 39
 Cordiner, M. A., Linnartz, H., Cox, N. L. J., et al. 2019, *ApJL*, 875, L28
 Cox, N. L. J. 2011, in *IAU Symp. 280, The Molecular Universe*, ed. J. Cernicharo & R. Bachiller (Cambridge: Cambridge Univ. Press), 162
 Cox, N. L. J., & Spaans, M. 2006, *A&A* 451, 973
 Cox, N. L. J., & Patat, F. 2008, *A&A*, 485, 9
 Cox, N. L. J., Cordiner, M. A., Cami, J., et al. 2006, *A&A*, 447, 991
 Cox, N. L. J., Boudin, N., Foing, B. H., et al. 2007, *A&A*, 465, 899
 Cox, N. L. J., Ehrenfreund, P., Foing, B. H., et al. 2011, *A&A*, 531, A25
 Dahlstrom, J., York, D. G., & Welty, D.E. 2013, *ApJ*, 773, 41
 Draine, B.T. 2011, *Physics of the Interstellar and Intergalactic Medium* (Princeton, NJ: Princeton Univ. Press)
 Ehrenfreund, P., Cami, J., Jiménez-Vicente, J., et al. 2002, *ApJL*, 576, L117
 Ellison, S. L., York, B. A., Murphy, M. T., Zych, B. J., Smith, A. M., & Sarre, P. J. 2008, *MNRAS*, 383, L30
 Fahlman, G. G., & Walker, G. A. H. 1975, *ApJ*, 200, 22
 Fitzpatrick, E. L., & Massa, D. 2007, *ApJ*, 663, 320
 Foing, B.H., & Ehrenfreund, P. 1994, *Nature*, 369, 296
 Friedman, S. D., York, D. G., McCall, B. J., et al. 2011, *ApJ*, 727, 33
 Fulara, J., Jakobi, M., & Maier, J.P. 1993, *Chem. Phys. Lett.*, 211, 227
 Galazutdinov, G. A., Manicó, G., & Krelowski, J. 2006, *MNRAS*, 366, 1075
 Hanson, M. M., Howarth, I. D., & Conti, P. S. 1997, *ApJ*, 489, 698
 Heckman, T.M., & Lehnert, M.D. 2000, *ApJ*, 537, 690
 Heger, M. L. 1922, *Lick Obs. Bull.*, 10, 146
 Hobbs, L. M., York, D. G., Snow, T. P., et al. 2008, *ApJ*, 680, 1256
 Hobbs, L. M., York, D. G., Thorburn, J. A., et al. 2009, *ApJ*, 705, 32
 Hoffmeister, V. H., Chini, R., & Scheyda, C. M. 2008, *ApJ*, 686, 310
 Jenniskens, P., Ehrenfreund, P., & Foing, B. 1994, *A&A*, 281, 517
 Junkkarinen, V. T., Cohen, R. D., Beaver, E. A., Burbidge, E. M., Lyons, R. W., & Madejski, G. 2004, *ApJ*, 614, 658
 Kos, J., & Zwitter, T. 2013, *ApJ*, 774, 72
 Krelowski, J., & Westerlund, B. E. 1988, *A&A*, 190, 339
 Krelowski, J. 2018, *PASP*, 130, 1001
 Lawton, B., Churchill, C. W., York, B. A., Ellison, S. L., Snow, T. P., Johnson, R. A., Ryan, S. G., & Benn, C. R. 2008, *AJ*, 136, 994
 Lewis, N. K., Cook, T. A., & Chakrabarti, S. 2005, *ApJ*, 619, 357
 Merrill, P. W. 1934, *PASP*, 46, 206
 Monreal-Ibero, A., Weilbacher, P. M., & Wendt, M. 2018, *A&A*, 615, 33
 Monreal-Ibero, A., Weilbacher, P. M., Wendt, M., et al. 2015, *A&A*, 576, 3
 Omont, A. 2016, *A&A*, 590, 52
 Phillips, M. M., Simon, J. D., Morrell, N., et al. 2013, *ApJ*, 779, 38
 Porceddu, I., Benvenuti, P., & Krelowski, J. 1992, *A&A*, 260, 391
 Povich, M. S., Churchwell, E., Biegging, J.H., et al. 2009, *ApJ*, 696, 1278
 Ramírez-Tannus, M. C., Cox, N. L. J., Kaper, L., & de Koter, A. 2018, *A&A*, 620, A52
 Ramírez-Tannus, M. C., Kaper, L., de Koter, A., et al. 2017, *A&A*, 604, 78
 Sarre, P. J. 2006, *J. Mol. Spec.*, 238, 1
 Snow, T. P., Jr., & Cohen, J. G. 1974, *ApJ*, 194, 313
 Snow, T.P., & McCall, B. J. 2006, *ARA&A*, 44, 367
 Sollerman, J., Cox, N., Mattila, S., et al. 2005, *A&A*, 429, 559

- Sonnentrucker, P. 2014, in IAU Symp. 297, The Diffuse Interstellar Bands, ed. J. Cami & N. L. J. Cox (Cambridge: Cambridge Univ. Press), 13
- Sonnentrucker, P., Cami, J., Ehrenfreund, P., & Foing, B.H. 1997, A&A, 327, 1215
- Sonnentrucker, P., York, B., Hobbs, L. M., et al. 2018, ApJS, 237, 40
- van Loon, J. Th., Bailey, M., Tatton, B. L., et al. 2013, A&A, 550, 108
- Vos, D. A. I., Cox, N. L. J., Kaper, L., Spaans, M., & Ehrenfreund, P. 2011, A&A, 533, 129
- Walker, G.A.H., Bohlender, D. A., Maier, J. P., & Campbell, E. K. 2015, ApJL, 812, L8
- Welty, D. E., Federman, S. R., Gredel, R., Thorburn, J. A., & Lambert, D.L. 2006, ApJS, 165, 138
- Welty, D. E., Ritchey, A. M., Dahlstrom, J.A., & York, D. G. 2014, ApJ, 792, 106
- Witt, A. N., Bohlin, R. C., & Stecher, T P. 1983, ApJL, 267, L47
- Xiang, F. Y., Li, A., & Zhong, J. X. 2011, ApJ, 733, 91
- Xiang, F. Y., Li, A., & Zhong, J. X. 2017, ApJ, 835, 107
- York, B. A., Ellison, S. L., Lawton, B., Churchill, C. W., Snow, T. P., Johnson, R. A., & Ryan, S. G. 2006, ApJL, 647, L29
- York, D. G., Dahlstrom, J., Welty, D. E., et al. 2014, in IAU Symp. 297, The Diffuse Interstellar Bands, ed. J. Cami & N. L. J. Cox (Cambridge: Cambridge Univ. Press), 89

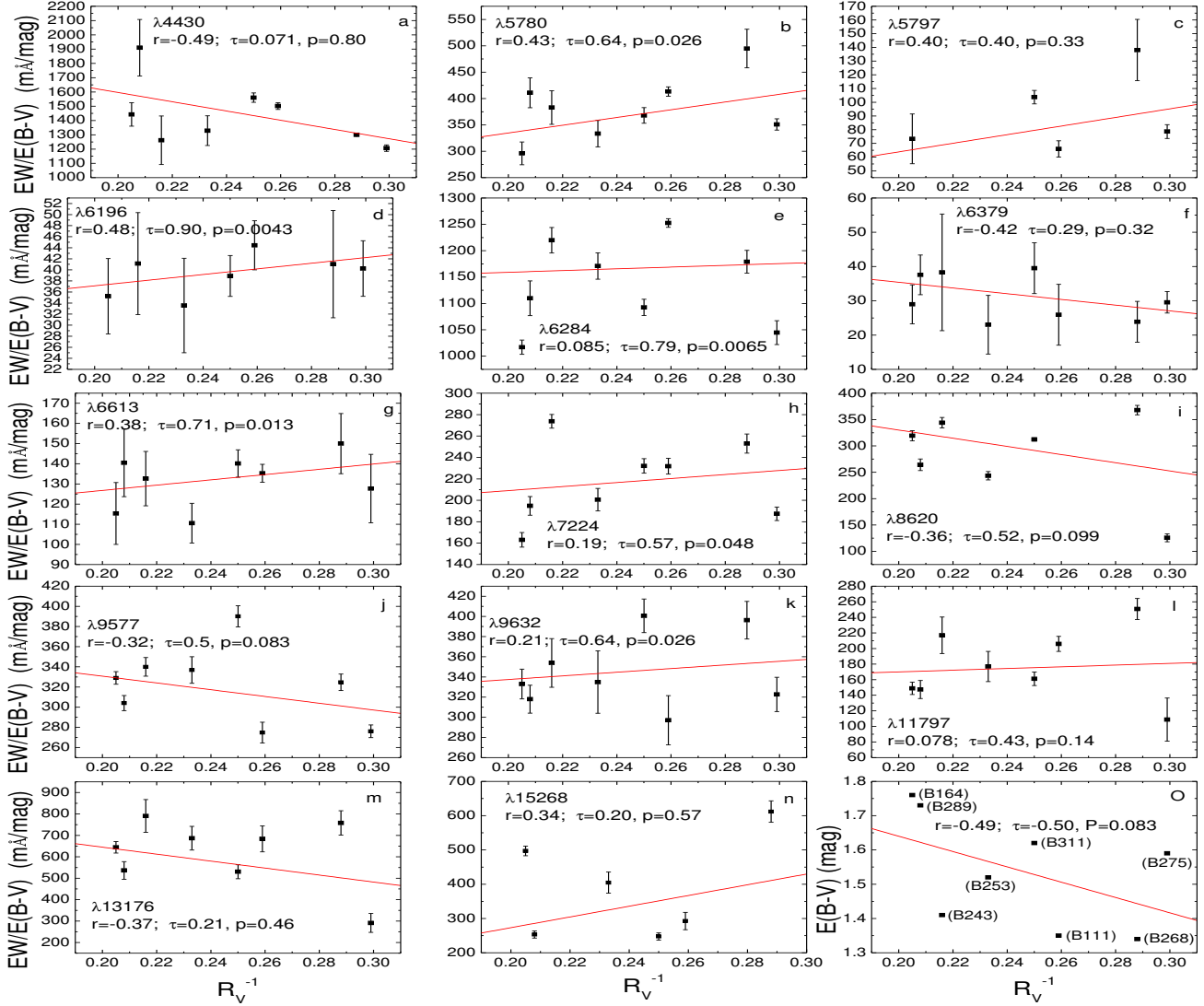


Figure 1. Correlation of the reddening-normalized DIB EW with R_V^{-1} for the lines of sight toward eight young OB stars in the giant H II region M17 for 14 DIBs at 4430 Å (a), 5780 Å (b), 5797 Å (c), 6196 Å (d), 6284 Å (e), 6379 Å (f), 6614 Å (g), 7224 Å (h), 8620 Å (i), 9577 Å (j), 9632 Å (k), 11797 Å (l), 13176 Å (m), and 15268 Å (n). Also shown is the correlation between the reddening $E(B-V)$ and R_V^{-1} (o). Labeled in each subfigure are the Pearson correlation coefficient r , the Kendall's τ coefficient and the significance level p . The star identifiers are also labeled in Figure 1(o).

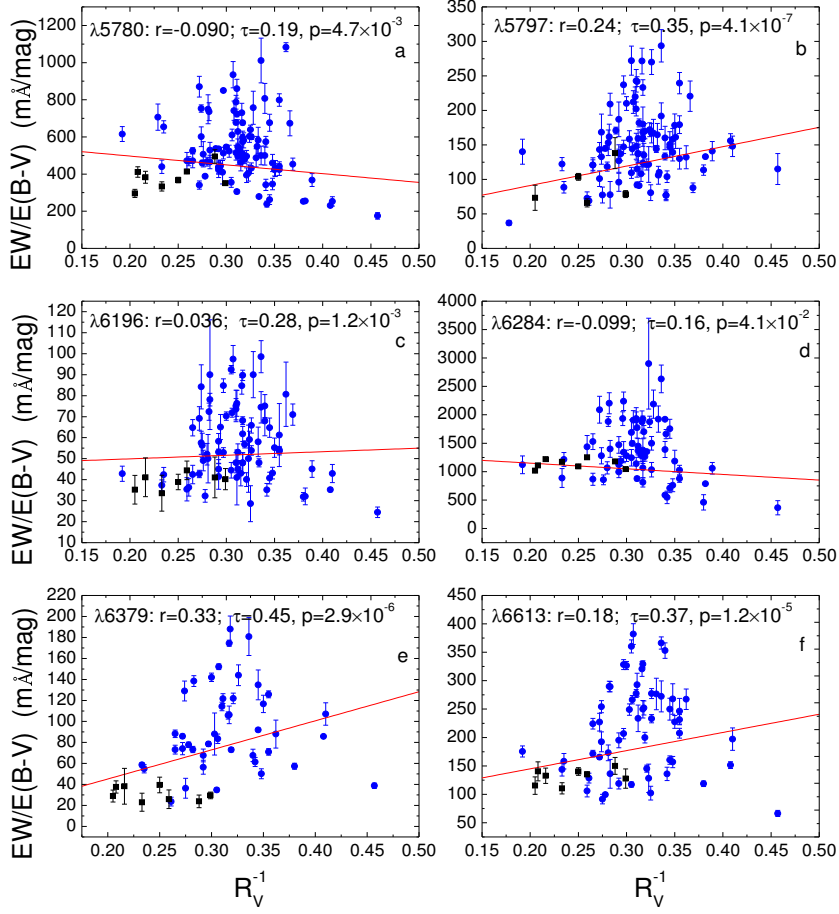


Figure 2. Correlation of the reddening-normalized DIB EW with R_V^{-1} for six DIBs at 5780 Å (a), 5797 Å (b), 6196 Å (c), 6284 Å (d), 6379 Å (e), and 6614 Å (f) for a large sample of 97 sightlines of which both EWs and R_V have been compiled from the literature by Xiang et al. (2017).

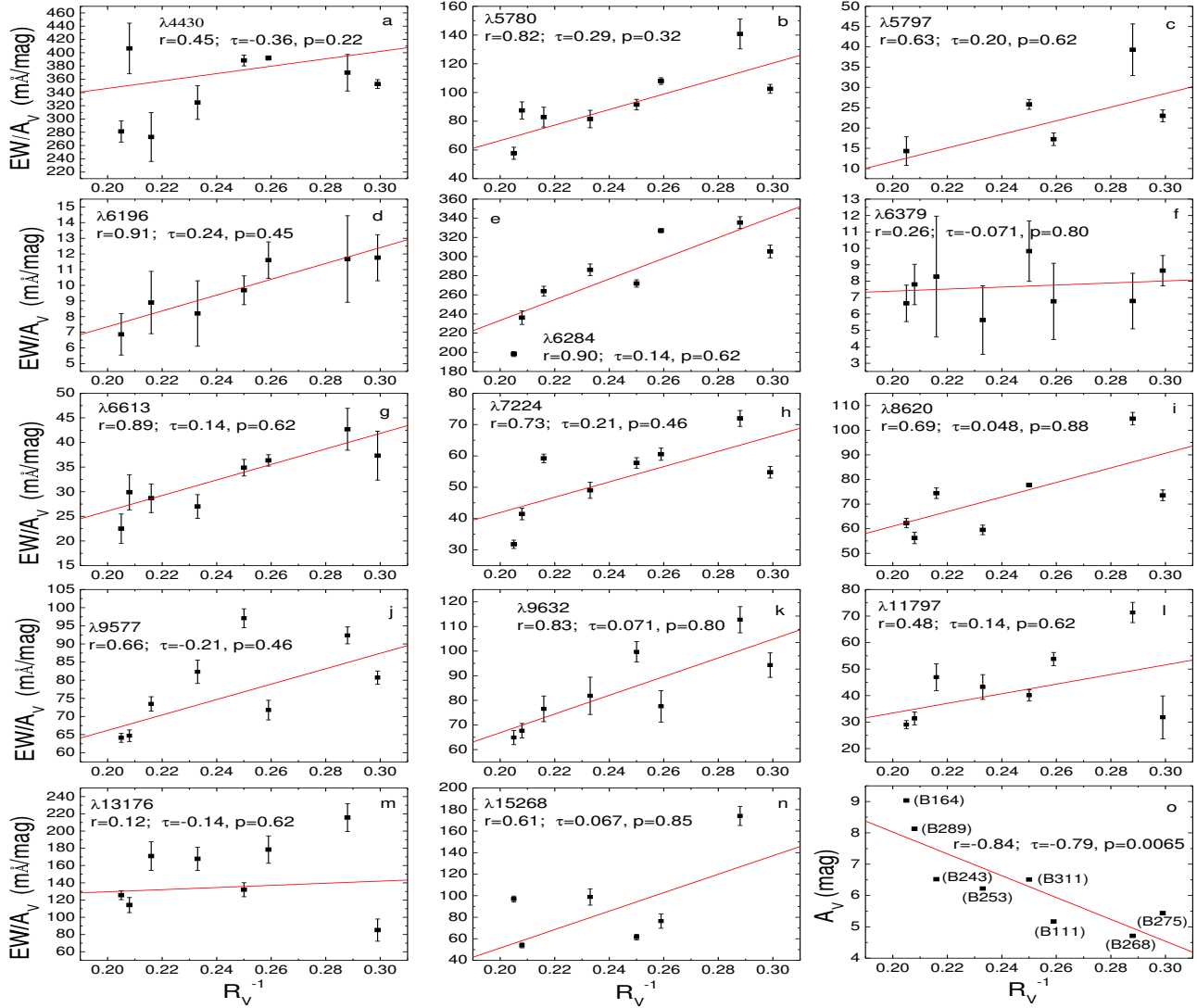


Figure 3. Same as Figure 1 but for EW/A_V , the extinction-normalized DIB EWs. Figure 3(o) shows the correlation between A_V and R_V^{-1} .

Table 1. Extinction and DIB Properties in the Lines of Sight toward Eight Young OB Stars (B111, B164, B243, B253, B268, B275, B289 and B311) in M17 (Ramírez-Tannus et al. 2018).

Extinction and DIB Properties	B111	B164	B243	B253	B268	B275	B289	B311
R_V	3.86	4.87	4.64	4.29	3.47	3.35	4.80	4.00
A_V /mag	5.17	9.03	6.52	6.22	4.71	5.44	8.13	6.51
$E(B - V)$ /mag	1.35	1.76	1.41	1.52	1.34	1.59	1.73	1.62
EW(4430)/mÅ	2027±32	2539±145	1779±240	2020±158	1742±130	1919±36	3304±311	2528±53
EW(5780)/mÅ	558±12	521±38	540±45	507±38	663±49	558±17	711±49	596±24
EW(5797)/mÅ	89±8	129±32	–	–	185±30	125±8	–	168±8
EW(6196)/mÅ	60±6	62±12	58±13	51±13	55±13	64±8	–	63±6
EW(6284)/mÅ	1691±11	1790±24	1720±34	1708±38	1580±29	1661±36	1920±57	1770±25
EW(6379)/mÅ	35±12	51±10	54±24	35±13	32±8	47±5	65±10	64±12
EW(6614)/mÅ	188±6	203±27	187±19	168±15	201±20	203±27	243±29	227±11
EW(7224)/mÅ	313±10	287±12	386±9	305±16	339±12	298±10	337±15	376±11
EW(8620)/mÅ	–	562±17	485±14	370±12	493±12	400±12	457±19	506±5
EW(9577)/mÅ	371±14	579±11	479±13	512±20	435±11	439±10	526±13	632±17
EW(9632)/mÅ	401±33	586±26	499±34	509±47	531±25	513±27	550±24	649±27
EW(11797)/mÅ	278±13	262±14	306±33	269±29	336±18	173±44	255±20	261±14
EW(13176)/mÅ	923±82	1134±47	1115±108	1044±84	1016±76	463±70	928±71	859±53
EW(15268)/mÅ	395±34	875±25	–	615±47	820±42	–	438±18	401±17